Transactions of the SMiRT 27
Yokohama, Japan, March 3-8, 2024
Division II *(Fracture Mechanics and Structural Integrity)*

EVALUATION OF HARMLESS CRACK SIZE ACCORDING TO THE STRESS RANGE R=(0 AND 0.4)

Kyoung-Hee Gu[1], Ki-Woo Nam[2], Kotoji Ando[3], Ye-Been Ji[4], Kwon-Hoo Kim[5]

[1] Graduate Student, Faculty of Engineering, Yokohama Nat'l Univ., Yokohama, Japan (rnrudgml6455@naver.com)
[2] Professor, Materials Science and Engineering, Pukyong Nat'l Univ., Busan, Korea (namkw@pknu.ac.kr)
[3] Emeritus professor, Faculty of Engineering, Yokohama Nat'l Univ., Yokohama, Japan (k_ando1943@yahoo.co.jp)
[4] Graduate Student, Dept. of Marine Design Engineering, Pukyong Nat'l Univ., Busan, Korea (wldpqls@naver.com)
[5] Professor, Metallurgical Engineering, Pukyong Nat'l Univ., Busan, Korea (mrppeng@pknu.ac.kr)

ABSTRACT

Since fatigue cracks usually initiate at the material surface, fatigue life is highly dependent on the surface condition. Surface cracks significantly decrease the fatigue limit. For the longevity of structures, it is necessary to improve fatigue life and make surface cracks harmless. In particular, it is necessary to examine the effect of the stress ratio. This study evaluated the effect of maximum stress ($\sigma_{m\,ax}$) and stress range ($\Delta\sigma$) according to the stress ratio (R=0 and 0.4) using the compressive residual stress of shot peened SUP9A. The threshold stress intensity factor ($\Delta K_{th(l)}$) obtained from CT specimen was constant regardless of stress ratio, but the $\Delta K_{th(l)}$ obtained from the applied stress ($\sigma_{m\,ax}$, $\Delta\sigma$) and fatigue limit of cracked specimen was different according to the stress ratio. The harmless crack size ($a_{hm\,l}$) using $\Delta K_{th(l)}$ from CT specimen was smaller (R=0) or greater (R=0.4) than that of $\Delta K_{th(l)}$ determined from the applied stress and fatigue limit of crack specimen. It was reasonable to evaluate the harmless crack size using the $\Delta K_{th(l)}$ and $\sigma_{m\,ax}$ obtained from CT specimen.

INTRODUCTION

Controlling defects in structures has been a long-standing research task related to fracture mechanics. Newman and Raju (1981) proposed a stress intensity factor evaluation equation for surface-cracked materials. This equation was used to predict the patterns of the surface-crack growth under tension or bending fatigue loads. Paris and Erdogan (1963) suggested a crack growth equation that provides the rate of growth of a fatigue crack. The stress intensity factor K characterizes the load around a crack tip, and the rate of crack growth was experimentally shown to be a function of the stress intensity range. Haddad et al. (1979) proposed an equation to evaluate the fatigue limit of microcracked materials. Kitagawa et al. (1976) experimentally demonstrated that the threshold stress intensity factor range (ΔK_{th}) of fatigue crack propagation for microcracks decreases as the crack length decreases. Tange et al. (1991) obtained a modified equation from Haddad's equation. This equation can be used to evaluate the dependence of the crack dimension of ΔK_{th} of a small crack when a semi-elliptical surface crack exists in a finite plate of stress ratio R. Ando et al. (2019) proposed a new ΔK_{th} evaluation equation for a small crack that focuses on nonlinear behavior at the fatigue limit, which is substantially lower than the yield stress. This equation analyzed the peculiar fatigue fracture behavior of the peened material by Ando et al. (2021)

Recently, a technique has been developed that can render harmless the surface cracks that reduce the fatigue limit by (20 to 60) % via the peening. (Houjou et al. (2013), Nakagawa et al. (2014), Takahashi et al. (2011, 2012, 2018), Yasuda et al. (2014)). Being rendered harmless or nondamaging surface cracks by peening is defined as "improving the fatigue limit of peened precracked materials to be 95 % or more of the fatigue limit of peened smooth materials". Several studies have been published on the fatigue fracture

behavior of peened cracked materials. However, there is no discussion on how surface crack nondamaging technique can affect the stress ratio for the maintenance and reliability improvement of steel components.

Therefore, this paper decided the threshold stress intensity factor by using the results of R=0.4 reported in a previous study, and verified the adaptability of Ando's equation (2019). At this time, the value of Yasuda et al. (2014) obtained from the CT specimen and the value determined from the fatigue limit of the cracked specimen were used for $\Delta K_{th(l)}$, and the maximum stress (σ_{max}) and stress range ($\Delta\sigma$) were used for the stress. That is, these values were used to evaluate the harmless crack size (a_{hml}). Using the results of the previous study, we assumed a crack depth (a_{NDI}) that could be accurately detected by nondestructive inspection. By comparing a_{hml} and a_{NDI}, rationalization and the improved reliability of maintenance of high-strength steel with a fatigue limit design were discussed under the stress range of stress ratios R=(0 and 0.4).

MATERIAL AND EXPERIMENT METHOD

The material and experimental method were based on Yasuda et al. (2014). The specimen with a plate width of 2W=10 mm and a thickness of t=3 mm was spring steel SUP9A, which was 470 HV by heat treatment. Figure 1 shows the shape and dimensions of the specimen and surface defects. Cyclic stresses were the plane-bending of the stress ratio R=(0 and 0.4). Crack was introduced into the semi-elliptical slit by electric discharge machining. The aspect ratio (As=a/c) was 1.0. Depth (a) was (0.1, 0.2, and 0.3) mm. For harmless cracking, shot peening was performed using a projection material having a diameter φ = 0.67 mm and a hardness of 600 HV. The specimen that was subjected to shot peening was called SP, while the specimen that was not subjected to shot peening was called Non-SP.

Fatigue tests were carried out on all specimens using a plane-bending fatigue testing machine. The fatigue test conditions were a stress ratio R=(0 and 0.4), and a cyclic frequency of 20 Hz. The stress waveform was a sine wave. The fatigue limit was defined as the maximum stress amplitude under which the specimen endured 10^7 cycles.

Figure 2 shows the residual stress distribution of the SP and non-SP specimens. The residual stress distributions in the thickness direction were measured from removing the surface layer by etching. The residual stress of Non-SP was almost zero. SP was a compressive residual stress in the outermost surface of $\sigma_{r,s}$=−550 MPa, with maximum compressive residual stress $\sigma_{r,max}$= −700 MPa.

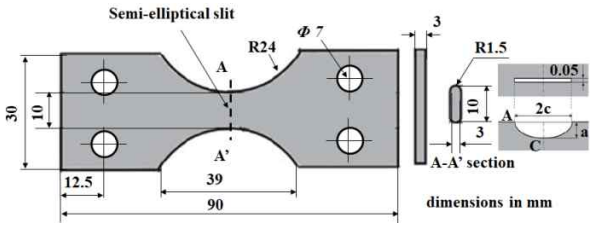

Fig. 1. Shape and dimension of specimen and surface defect.

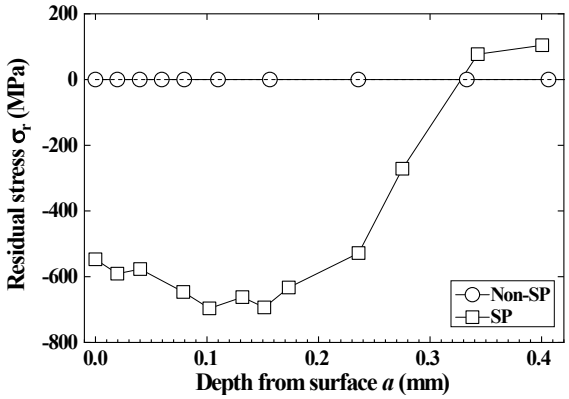

Fig. 2. Residual stress distribution by SP and Non-SP specimen.

ANALYSIS METHOD

The crack length dependence of the threshold stress intensity factor range (ΔK_{th}) of the fatigue crack propagation proposed by the authors can be evaluated using Eq. 1. (Ando et al. (2019))

$$\Delta K_{th} = 2\beta\Delta\sigma_w\sqrt{\frac{a}{\pi}}\cos^{-1}\left[\left\{\frac{\pi}{8\beta^2 a}\left(\frac{\Delta K_{th(l)}}{\Delta\sigma_w}\right)^2+1\right\}^{-1}\right] \quad (1)$$

where, $\Delta K_{th(s)}$ and $\Delta K_{th(l)}$ are the threshold stress intensity factor ranges of the fatigue crack propagation of small cracks and sufficiently large cracks, respectively; $\Delta\sigma_w$ is the fatigue limit (range) of the smooth specimen, and when $R \geq 0$, $\Delta\sigma = \sigma_{max} - \sigma_{min}$, as shown in Figs. 3(a) and (b). The $\Delta\sigma$ is the applied stress range; a is the depth of the semielliptical crack, and β is the shape correction factor given by the Newman–Raju equation (Newman and Raju (1981)) at the deepest crack point when the specimen of the finite plate is subjected to a bending stress. The β of the outermost surface is substituted by c.

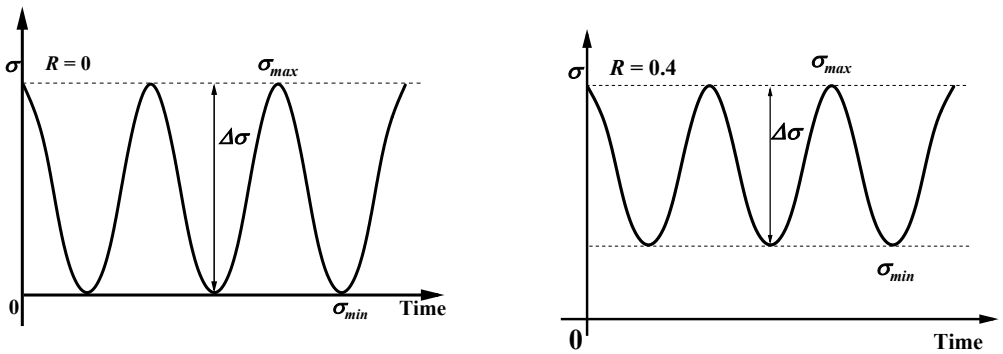

Fig. 3. Definition of stress in the case of stress ratio R=(0 and 0.4) ($\Delta\sigma = \sigma_{max} - \sigma_{min}$).

The harmless crack size by shot peening can be evaluated based on fracture mechanics. In this study, we used Eq. (2) to evaluate the apparent stress intensity factor range, ΔK_{Tr}, assuming that the positive value of the stress intensity factor contributes to fatigue crack propagation:

$$\Delta K_{Tr} = \Delta K_{sp} + K_r \quad (2)$$

where, ΔK_{sp} is the stress intensity factor range of $\Delta\sigma_{sp}$; this is evaluated by the Newman–Raju equation. The K_r is the stress intensity factor obtained from the residual stress distribution shown in Fig. 2 based on the API method (2000).

The harmless crack is a condition where the sum ΔK_{Tr} of ΔK_{sp} of surface crack length or depth and K_r by residual stress is equal to or less than $\Delta K_{th(s)}$. That is, the condition of harmless crack size (a_{hlm}) of the SP specimen is $\Delta K_{Tr} \leq \Delta K_{th}$. The conditions of a_{hlm} were compared with the deepest crack point and outermost surface. A smaller crack size is defined as a harmless crack (a_{hlm}).

RESULTS AND DISCUSSION

Yasuda et al. (2014) determined $\Delta K_{th(l)}$ to be 7.5 MPa$\sqrt{\text{m}}$ obtained by the gradual decrease test for a compact tension specimen of SUP9A. However, the fatigue limit ($\Delta\sigma_w$) of non-SP cracked specimen was (400, 360, and 280) MPa at R=0, and (400, 320, and 240) MPa at R=0.4, meaning that the fatigue limit was different at crack depth. In the case of R=0.4, only the stress ($\Delta\sigma$) of 60 % of the fatigue limit (=$\sigma_{m\,ax}$) affects the propagation of the crack. Hence, 60 % of the fatigue limit was applied for the evaluation. Therefore, it is necessary to accurately determine $\Delta K_{th(l)}$ based on the fatigue limit result according to the applied stress range ($\Delta\sigma$).

Figures 4(a) and (b) show that $\Delta K_{th(l)}$ is determined in the fatigue limit according to the applied stress range at the different stress ratio. At this time, $\Delta K_{th(l)}$was examined between (5.42 ~ 6.37) MPa$\sqrt{\text{m}}$ and (5.21 ~ 6.10) MPa$\sqrt{\text{m}}$ for fatigue limit ($\Delta\sigma_w$= 840 and 680 MPa) of smooth specimen at R=(0 and 0.4), respectively. The $\Delta K_{th(l)}$ was evaluated using Eq. (1).

Figure 4 (a) shows the results at R=0. This was evaluated by crack depth. In detail, the 0.2 mm portion was between fracture and not-fracture, while the (0.1 and 0.3) mm portions were in the not-fracture portion. However, overall, it was judged that the most suitable $\Delta K_{th(l)}$ was 6.37 MPa$\sqrt{\text{m}}$. Figure 4(b) shows the results at R=0.4. These results agreed well with the experimental results. In general, $\Delta K_{th(l)}$ was found to be optimal at 5.65 MPa$\sqrt{\text{m}}$.

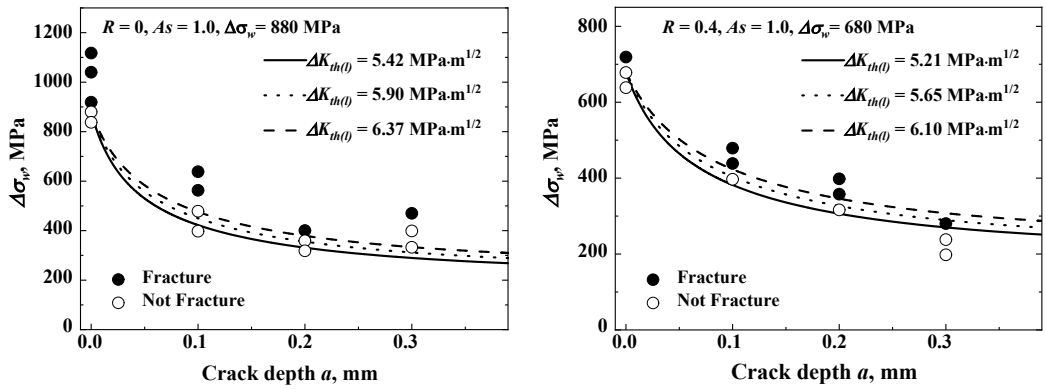

(a) (b)

Fig. 4. Fatigue limit and crack relation to determine the threshold stress intensity factor. (a) R =0, (b) R =0.4.

Table 1 shows the $\Delta K_{th(l)}$ determined from Yasuda et al. (201) and Fig. 4, where, Nos. ① and ②, and Nos. ③ and ④, are characteristic values of R=(0 and 0.4), respectively; $\Delta\sigma_w$ and $\Delta\sigma_{sp}$ are the fatigue limit of smooth specimen and SP smooth specimen, respectively; and $\Delta K_{th(l)}$ is the threshold stress intensity factor of large cracks.

Table 1 $\Delta K_{th(l)}^{R}$ obtained from Yasuda et al. (2014) and Fig. 4.

No.	R	$\Delta\sigma_w$ (MPa)	$\Delta\sigma_{sp}$ (MPa)	$\Delta K_{th(l)}$ (MPa$\sqrt{\text{m}}$)	
①	0	880	960	6.37	Determined from fatigue limit of cracked specimen
②	0	880	960	7.5	Ref. 12
③	0.4	680	600	5.65	Determined from fatigue limit of cracked specimen
④	0.4	1,133	1,000	7.5	Ref. 12

Figures 5 and 6 show the relationship between the stress intensity factor range $\Delta K_{Tr(A,C)}$ obtained from the deepest portion and surface respectively, and the crack depth a of semi-elliptical cracks with R=(0 and 0.4). The $\Delta K_{Tr(A,C)}$ is the sum of ΔK_{sp} obtained from Newman–Raju's equation (1981), and K_r obtained from API−RP579 (2000). This was obtained from Eq. (2). The threshold stress intensity factor range $(\Delta K_{th(s)A,C})$ was obtained from Eq. (1).

In Fig. 5, $\Delta K_{th(s)A}$ and $\Delta K_{th(s)C}$ were obtained by substituting 880 MPa and (6.37 or 7.5) MPa$\sqrt{\text{m}}$ into $\Delta\sigma_w$ and $\Delta K_{th(l)}$, respectively, in Eq. (1). The crossing point of $\Delta K_{Tr(A,C)}$ and $\Delta K_{th(s)A,C}$ is a=(0.152 and 0.255) mm at $\Delta K_{th(l)}$=(6.37 and 7.5) MPa$\sqrt{\text{m}}$, respectively. The crossing point using $\Delta K_{th(l)}$=7.5 MPa$\sqrt{\text{m}}$ of Yasuda et al. (2014) was greater than that of $\Delta K_{th(l)}$=6.37 MPa$\sqrt{\text{m}}$ determined from the fatigue limit of cracked specimen. This means that a crack less than the depth of the crossing point can be harmless. In addition, in Yasuda et al. (2014), a=0.2 mm was harmless, but a=0. mm was not. From this, in the case of R=0, it is reasonable to evaluate the harmless crack size using the $\Delta K_{th(l)}$ obtained from the CT specimen.

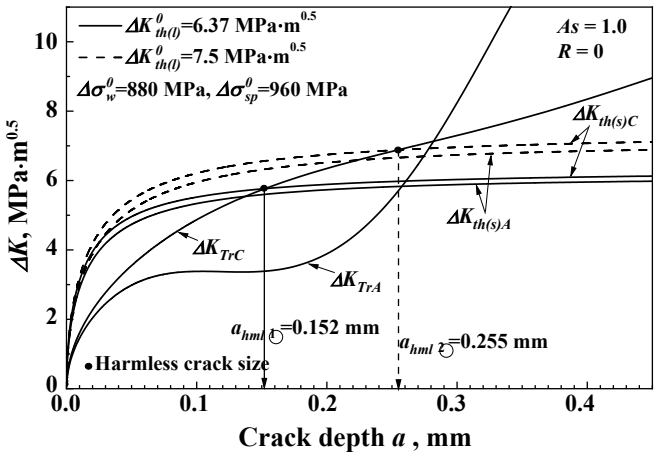

Fig. 5. Evaluation of harmless crack size using the $\Delta K_{th(l)}$ of Yasuda et al. (2014) and $\Delta K_{th(l)}$ obtained from the fatigue limit of cracked specimen at R=0.

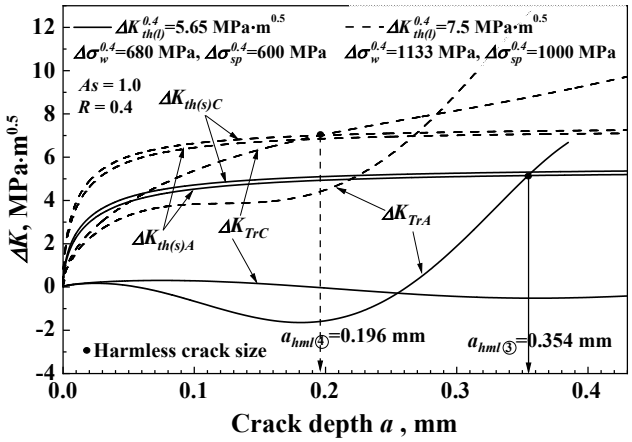

Fig. 6. Evaluation of the harmless crack size using the $\Delta K_{th(l)}$ of Yasuda et al. (2014) and the $\Delta K_{th(l)}$ obtained from the fatigue limit of cracked specimen at *R*=0.4.

The $\Delta K_{th(s)A}$ and $\Delta K_{th(s)C}$ in Fig. 6 were evaluated with two stresses. One was the maximum stress ($\sigma_{m\,ax}$), while the other was the stress range ($\Delta\sigma$) of *R*=0.4. That is, $\Delta K_{th(s)A}$ and $\Delta K_{th(s)C}$ were obtained by substituting in Eq. (1) the following values, respectively: $\Delta\sigma_w$=1,133 MPa and $\Delta K_{th(l)}$=7.5 MPa$\sqrt{\text{m}}$ obtained from Yasuda et al. (2014); and $\Delta\sigma_w$=680 MPa and $\Delta K_{th(l)}$=5.65MPa$\sqrt{\text{m}}$ determined from the fatigue limit of crack specimen. The crossing point of $\Delta K_{Tr(A,C)}$ and $\Delta K_{th(s)A,C}$ is *a*=(0.196 and 0.354) mm at $\Delta K_{th(l)}$=(7.5 and 5.65) MPa$\sqrt{\text{m}}$, respectively. The crossing point using $\Delta K_{th(l)}$=5.65 MPa$\sqrt{\text{m}}$ determined from the fatigue limit of cracked specimen was greater than that of $\Delta K_{th(l)}$=7.5 MPa$\sqrt{\text{m}}$ of Yasuda et al. (2014). This is because $\Delta K_{th(l)}$ and $\Delta\sigma$ are small. In Yasuda et al. (2014), *a*=0.2 mm of *R*=0.4 was harmless, but *a*=0.3 mm was not. From this, in the case of *R*=0.4, it is reasonable to evaluate the harmless crack size using the $\Delta K_{th(l)}$ obtained from the CT specimen and the maximum stress ($\Delta\sigma_{m\,ax}$) of the fatigue limit.

The crack depths at fatigue limit reduction rates of (25 and 50) % in a smooth specimen are defined as a_{25} and a_{50}, respectively. The two nondestructive inspections were assumed by ultrasonic detection with the highest probability of fatigue crack detection (Gu et al. (2023)). *NDI1* assumed a semi-elliptical crack with 2*c* and *a* of (0.6 and 0.3) mm, respectively. The area and depth of this crack are S_{NDI1} and a_{NDI1}, respectively. *NDI2* assumed that a crack with 60 % detection probability had 2*c* and *a* of (1.4 and 0.25) mm, respectively. The area and depth of this crack are S_{NDI2} and a_{NDI2}, respectively. The area (*S*) of a semi-elliptical crack can be obtained using *S*=*πac/2*. Thus, for the same *S* of a semi-elliptical crack, the detection probability of the crack will be the same, independent of *As*. The relationship between a_{NDI} and *As* is evaluated using Eq. (3):

$$S_{NDI} = \pi {a_{NDI}}^2/2As \tag{3}$$

Figures 7(a) and (b) show the *As* dependence of a_{hm} by *SP* in *R*=(0 and 0.4), respectively. In the (a) *R*=0, the $a_{hm\,①}$ was determined at the crack surface (*As*=1.0, 0.7, 0.4) or depth (*As*=0.1). The $a_{hm\,②}$ was determined at the crack surface (*As*=1.0, 0.7) or depth (*As*=0.4, 0.1). It was observed that $a_{hm\,l}$ increased with *As*. The $a_{hm\,①}$ was determined at smaller than $a_{hm\,②}$. This is because the applied stress ($\Delta\sigma_w$, $\Delta\sigma_{sp}$) and residual stress substituted in Eqs. (1) and (2) are the same, but the $\Delta K_{th(l)}$ determined from the fatigue limit of the cracked specimen is small. Meanwhile, all the $a_{hm\,③}$ values of *R*=0.4 were determined at the crack depth. The $a_{hm\,④}$ was determined at the crack surface (*As*=1.0, 0.7) or depth (*As*=0.4, 0.1). It was also observed that $a_{hm\,l}$ increased with *As*. The $a_{hm\,③}$ was greater than $a_{hm\,④}$. This is because the residual substituting in Eq. (2) is the same, but the applied stress ($\Delta\sigma_w$, $\Delta\sigma_{sp}$) and the

$\Delta K_{th(l)}$ determined from the fatigue limit of the cracked specimen are different. As mentioned above, it is reasonable to evaluate $a_{hm\,l}$ using the $\Delta K_{th(l)}$ obtained in the experiment and s_{max}, regardless of the *R*.

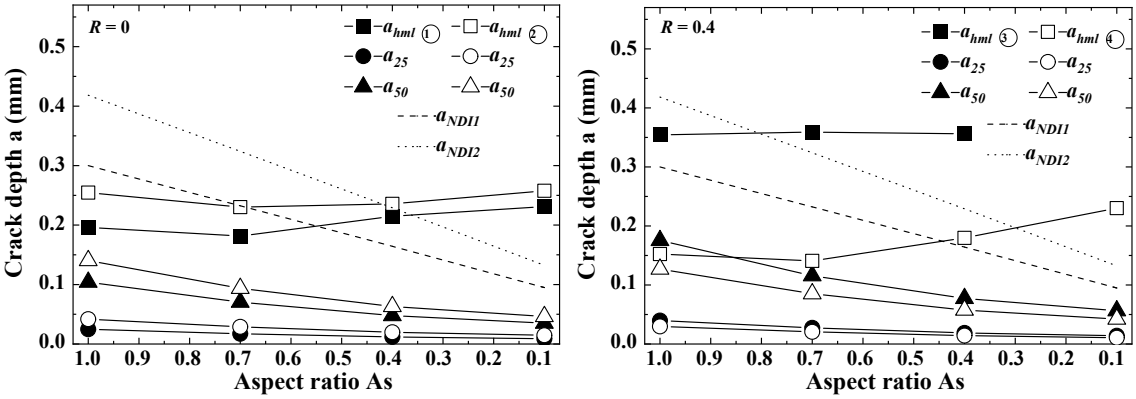

(a) (b)

Fig. 7. *As* dependence of harmless available crack depth ($a_{hm\,l}$), a_{25}, a_{50} and a_{NDI}. (a) *R*=0, (b) *R*=0.4.

Figures 7(a) and (b) show the crack depths (a_{25}, a_{50}), which reduce the fatigue limit of a non-*SP* smooth material by 25 % (a_{25}) and 50 % (a_{50}). Furthermore, Fig. 7 shows the relationship between *As* and each of (a_{NDI1}, a_{NDI2}), which can be determined using the *NDI* method expressed in Eq. (3). Figures 7(a) and (b) show the results for *R*=(0 and 0.4), respectively. It was observed that the crack depths increased with *As*. The cracks with a depth of a_{25} and a_{50} can be rendered harmless, because the crack depth (a_{25}, a_{50}) was below the harmless crack size ($a_{hm\,①}$ ■, $a_{hm\,②}$ □), regardless of $\Delta K_{th(l)}$ and *R*.

We discussed the crack detection ability (a_{NDI1}, a_{NDI2}). As presented in Figs. 7(a) and (b), the crack detection ability (dashed and dotted line) is above the fatigue crack (a_{25}, a_{50}), which indicates that the *NDI* could not detect cracks with a depth of a_{25} and a_{50}. Hence, a higher resolution *NDI* technology is needed.

CONCLUSIONS

This study evaluated the *As* dependence of $a_{hm\,l}$ by *R*=(0 and 0.4), and the *As* dependence of crack depth (a_{25}, a_{50}) that reduces the fatigue limit of non-SP smooth material by (25 or 50) %. The harmless crack size ($a_{hm\,l}$) evaluated the effect of maximum stress (σ_{max}) and stress range ($\Delta\sigma$) according to the stress ratio. In addition, the detection limits (a_{NDI1}, a_{NDI2}) of fatigue cracks via NDI were assumed, and the detection ability of cracks that reduced the fatigue limit was evaluated. The results obtained were as follow:

(1) The threshold stress intensity factor ($\Delta K_{th(l)}$) obtained from CT specimen was 7.5 MPa$\sqrt{\text{m}}$, regardless of stress ratio. However, the $\Delta K_{th(l)}$ values obtained from the applied stress (σ_{max}, $\Delta\sigma$) and the fatigue limit of cracked specimen were different, according to the stress ratio. $\Delta K_{th(l)}$ was 6.37 MPa$\sqrt{\text{m}}$ for *R*=0, and $\Delta K_{th(l)}$ was 5.65 MPa$\sqrt{\text{m}}$ for *R*=0.4.

(2) The $a_{hm\,l}$ using $\Delta K_{th(l)}$ obtained from CT specimen was smaller (*R*=0) or greater (*R*=0.4) than that of $\Delta K_{th(l)}$ determined from the fatigue limit of cracked specimen. However, $a_{hm\,l}$ using the σ_{max} and the $\Delta K_{th(l)}$ obtained from the CT specimen showed good agreement with the $a_{hm\,l}$ of the experiment. Therefore, it was reasonable to evaluate the harmless crack size using $\Delta K_{th(l)}$ and σ_{max} from CT specimen.

(3) The cracks with depth of a_{25} and a_{50} can be rendered harmless, because the crack depth (a_{25}, a_{50}) was below the harmless crack size ($a_{hm\,①}$, $a_{hm\,②}$), regardless of $\Delta K_{th(l)}$ and *R*.

(4) The crack detection ability (a_{NDI}) is above the fatigue crack (a_{25}, a_{50}), which indicates that the *NDI* could not detect cracks with a depth of a_{25} and a_{50}. Hence, a higher resolution *NDI* technology is needed.

REFERENCES

American Petroleum Institute (API). (2000). "Fitness-for-Service," 1st Ed. American Petroleum Institute.

Ando, K., Fueki, R., Nam, K. W., Matsui, K., Takahashi, K. (2019). "Study on the unification of the threshold stress intensity factor for micro crack growth," *Transactions of JSSE,* 64 39-44.

Ando, K., Kim, M. H., Nam, K. W. (2021). "Analysis on peculiar fatigue fracture behavior of shot peened metal using new threshold stress intensity factor range equation," *Fatigue Fract Eng Mater Struct.,* 44 306-316.

EI Haddad, M. H., Topper, T. H., Smith, K. N. (1979). "Prediction of non-propagating cracks," *Eng Fract Mech*., 11 573-584.

Gu, K. H., Ando, K., Nam, K. W. (2023). "Analytical study on rationalize and reliability improvement of maintenance against stress corrosion cracking in stainless steel welds of LWR primary system," Journal of Mechanical Science and Technology, 37 1773-1780.

Houjou, K., Takahashi, K., Ando, K. (2013). "Improvement of Fatigue Limit by Shot Peening for High-Tensile Strength Steel Containing a Crack in the Stress Concentration Zone," International Journal of Structural Integrity, 4 258-266.

Kitagawa, H, Takahashi, S. (1976). "Applicability of fracture mechanics to very small cracks or the cracks in the early stage," *In: Proc. 2nd Intern. Conf. Mech. Behav. Mater.*, *Boston, ASM, Cleveland, Ohio,* 627–631.

Nakagawa, M., Takahashi, K., Osada, T., Okada, H., Koike, H. (2014). "Improvement in Fatigue Limit by Shot Peening for High-strength Steel Containing Crack-like Syrface Defect (Influence of Surface Crack Aspect Ratio)," Transactions of Japan Society of Spring Engineers, 2014 13-18.

Newman, Jr. J. C., Raju, I. S. (1981). "An empirical stress-intensity factor equation for the surface crack," *Eng Fract Mech*., 15 185-192.

Paris, P. C., Erdogan, F. (1963). "A Critical Analysis of Crack Propagation Laws," Journal of Basic Engineering, 85 528-533.

Tange, A., Akutu, T., Takamura, N. (1991). "Relation between shot-peening residual stress distribution and fatigue crack propagation life in spring steel," *Transactions of JSSE,* 19 47-53.

Takahashi, K., Amano, T., Ando, K., Takahashi, F. (2011). "Improvement of Fatigue Limit by Shot Peening for High-Strength Steel Containing a Crack-like Surface Defect," International Journal of Structural Integrity, 2 281-292.

Takahashi, K., Okada, H., Ando, K. (2012). "Effects of Shot Peening on the Torsional Fatigue Limit of High-Strength Steel Containing an Artificial Surface Defect," International Journal of Structural Integrity, 3 274-284.

Takahashi, K., Osedo, H., Suzuki, T., Fukuda, S. (2018). "Fatigue Strength Improvement of an Aluminum Alloy with a Crack-Like Surface Defect Using Shot Peening and Cavitation Peening," Engineering Fracture Mechanics, 193 151-161.

Yasuda, J., Takahashi, K., Okada, H. (2014). "Improvement of Fatigue Limit by Shot Peening for High-Strength Steel Containing a Crack like Surface Defect -Influence of Stress Ratio-," International Journal of Structural Integrity, 5 45-59.